GlueX-doc-742
CVS: docs/momres_cdc
Original: January 31, 2007
Update: February 13, 2007

Parametric Momentum Resolution in the Central Drift Chambers

D. Lawrence and E.S. Smith

1 Introduction

The momentum resolution in the Central Drift Chambers (CDC) can be determined parametrically using the program MOMRES [1, 2]. This program is limited in that it only works in two-dimensions and therefore cannot be used to address general resolution issues in the Hall D detector. However, it is ideally suited to estimate the resolution of momentum, angles and vertex resolution for particles emitted at 90 degrees from the target and registered in the CDC straw tube chambers. It therefore provides a check on full reconstruction in special cases, can verify correctness of geometry files, and can help identify additional contributions to the resolution due to track finding and fitting procedures. This program can also be easily used for systematic studies of various types using the CDC geometry for comparison with results obtained with HDFAST [3, 4].

2 Usage of MOMRES

The program MOMRES was written by Bernhard Mecking based on the reference trajectory method [1]. The output format of the program was updated for simulations of the CLAS12 detector [2]. We have made a few modifications to the code for ease simulations of tracking inside the Hall D solenoidal magnet. Note that the beam direction is along the x-axis. The material and measurement points along a trajectory are specified in the input file "momres.dat," examples of which are shown in the appendix. The file specifies the particle mass and range of momenta to be considered. It then contains a table with one line per layer of material in the detector. Each line specifies the step size for use in that material, end position relative to the target (assumes material fills the volume since the previous listed position), the resolution (σ) of a position measurement (blank if the material is inactive), the radiation length of the material, and a descriptive comment. The units are meters. The version of the program we have used uses a uniform magnetic field along the axis of the solenoid (z-axis), although the program allows for a field map to be read from a file. We have used the nominal field of 1.74 T in the solenoid radially outward from the center of the Hall D target.

3 Materials in the CDC

The material assumed for the target and other materials surrounding the target is given in Table 1. The material inside the CDC active volume is 2.1% of X_0 for particles traveling radially outward. The material in the CDC active volume is 4.9% of X_0. A plot of the material as a function of radius is shown in Fig. 1. A model for three additional layers of CDC inside the nominal radius is shown in Fig. 2. Although the forward drift chamber system is not treated here, for reference we include the material list for those chambers in Appendix **??**.

Table 1: Material thickness in the CDC for particles traversing perpendicular to the chamber. Note that the wire and straw tube entries are averaged over the volume of one cell.

Layer	Material	Density (g/cm^3)	Thick (cm)	Thick (g/cm^2)	X0 (cm)	X0 (g/cm^2)	x/X0
Target	H	0.0708	1.5	0.1062	866.0	61.31	0.0017
Target cell wall	Kapton	1.42	0.016	0.0220	28.6	40.612	0.0006
Rohacell scat chamb	PMI	0.1100	1	0.11	373.1	41.04	0.0027
Start counter	PVT	1.03	0.388	0.4	40.8	42	0.0095
CDC inner shell	Al	2.7	0.06	0.162	8.9	24.03	0.0067
CDC Straw Tubes	Kapton/Al	0.0258	43.6	1.1236	1483.8	38.24	0.0294
CDC gas	A/CO_2	0.0013	43.6	0.05856	19173.1	25.75	0.0023
CDC outer shell	Fiberglass	1.9100	0.6	1.146	22.0	42	0.0273
CDC thickness (23 layers)		0.0271	43.6	1.182	1377.2	37.34	0.0317
Thickness per layer		0.0271	1.896	0.051	1377.2	37.34	0.0014
End plate	Al	2.7	0.6	1.62	8.9	24.03	0.0674

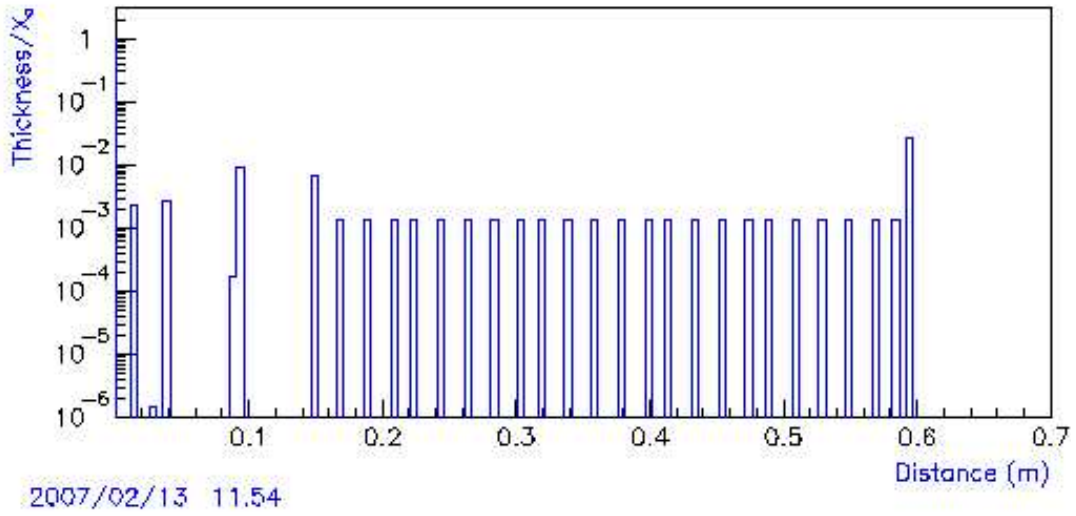

Figure 1: Distribution of material in the CDC radially outward for the nominal 23-layer configuration. This configuration includes the hydrogen target, scattering chamber and start counter inside the CDC.

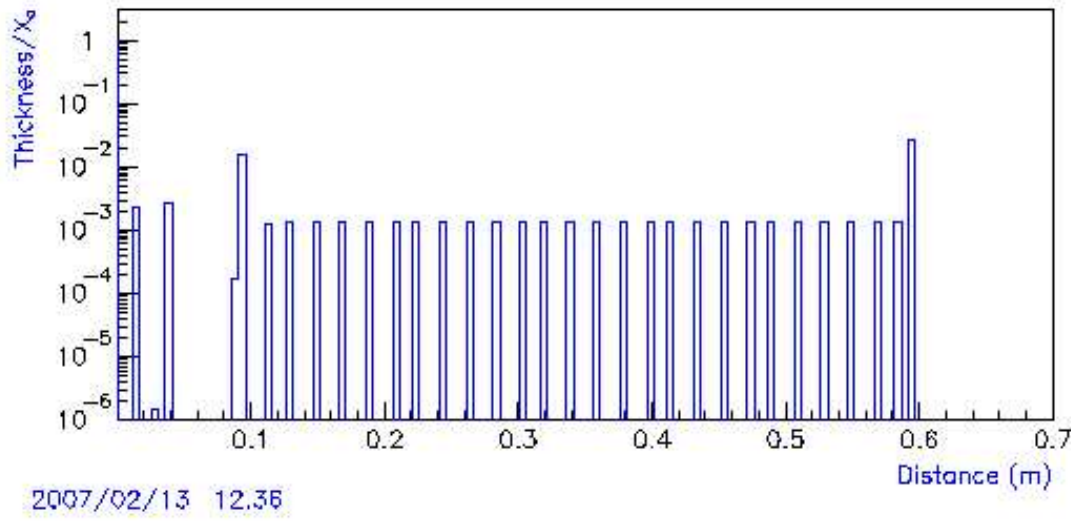

Figure 2: Distribution of material in the CDC radially outward which extends the normal configuration by adding 3 layers between the start counter and the nominal inner radius of the detector. Resolutions were computed for configuration with different number of layers by omitting intermediate layers.

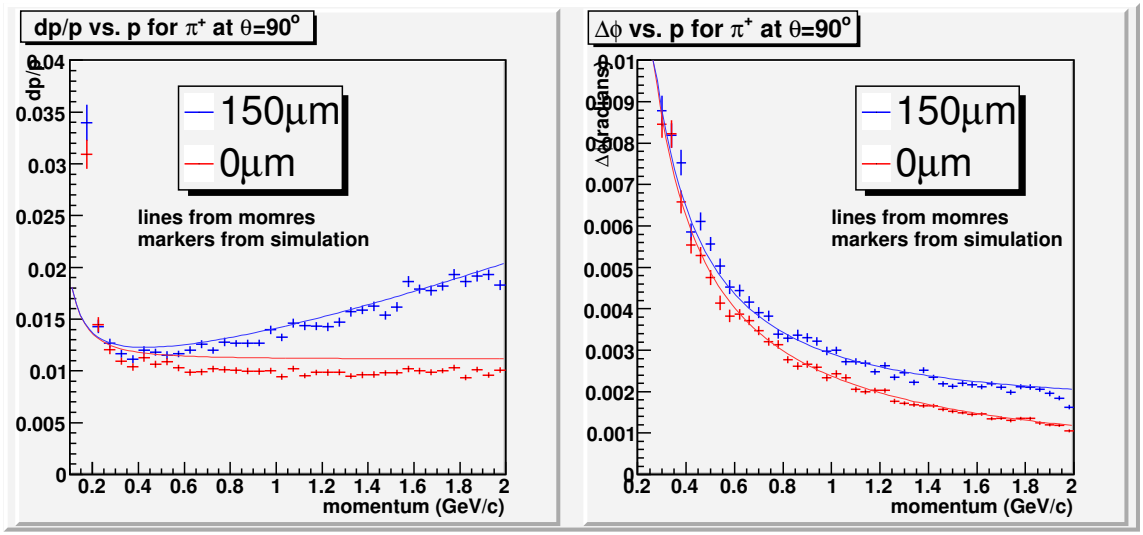

Figure 3: Comparison of the parametric resolution for pions between MOMRES and the GlueX track reconstruction program. Note that this comparison is made for B = 1.74 T, which is the nominal average field in the solenoid at 90°.

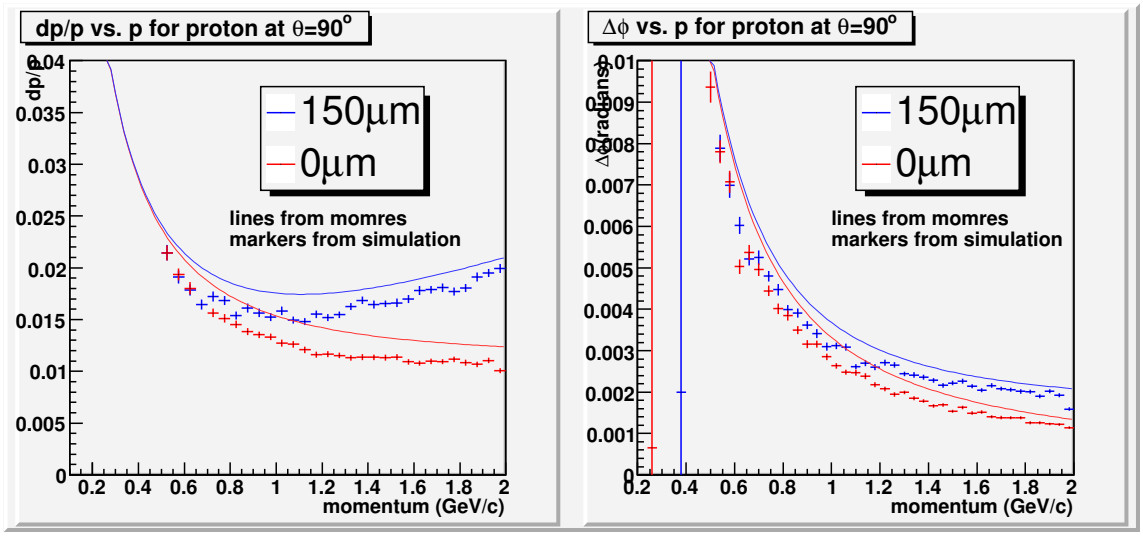

Figure 4: Comparison of the parametric resolution for protons between MOMRES and the GlueX track reconstruction program. Note that this comparison is made for B = 1.74 T, which is the nominal average field in the solenoid at 90°.

4 Comparison of parametric results with full reconstruction

We have compared the results of the momentum and angular resolution obtained with MOMRES with the tracking reconstruction from GlueX [5]. The results are shown in Fig. 3 and 4. This comparison is made at a B = 1.74 T, which is the nominal average field in the solenoid at 90°. The GlueX reconstruction predicts a 20% smaller contribution due to multiple scattering. One of the differences between this parametric approach and the full simulation is due to the effective thickness of the straws in the GEANT geometry file which is matched to the weight of the Kapton/Al combination, not to its radiation length. The true radiation length of the combination is approximately 8% higher, which would increase the GlueX simulation contribution from multiple scattering by about 4%. The geometry of the two configurations is also not exactly the same, which may also lead to some differences. Finally, for an exact comparison one should check that the root-mean-square multiple scattering angles, for which there are can be different approaches, are the same between the two simulations.

5 Parameterization of resolution at 90°

The resolution was computed for pions and protons and the decomposition of the fractional momentum resolution, angular resolution and vertex resolutions are shown in Fig. 5 and 6 using the material specified in Appendix A and the nominal position resolution of Fig. **??**. The resolution for pions assuming a degraded position resolution of $\sigma = 300\mu m$ is shown in Fig. 7. It confirms that the position terms are proportional to the CDC measurement error, and the multiple scattering terms are unaffected by the measurement uncertainties. Using this ansatz, we have plotted the resolutions in the CDC as a function of measurement errors in Fig. 8. These plots show that little improvement is obtained in reducing the position resolution below the nominal value of $\sigma = 150\mu m$.

6 Reducing material inside CDC

The start counter surrounding the target will be used in the early phases of Hall D running for ease of triggering at Level 1. However, as the detector is operated at higher rates, the start counter will become less effective at reducing background and the triggering load will move to the Level 3 software trigger. At that time, the start counter will be removed to reduce the material between the tracking system and the target. This configuration, shown in Fig. 11, should be used as a reference for determining the ultimate limitations that can be obtained from the tracking system. Compared to the nominal setting (Fig. 5), the fractional momentum resolution is unchanged, as expected. The position contributions to the angular and vertex resolutions are unchanged, and the contributions due to multiple scattering to the angular

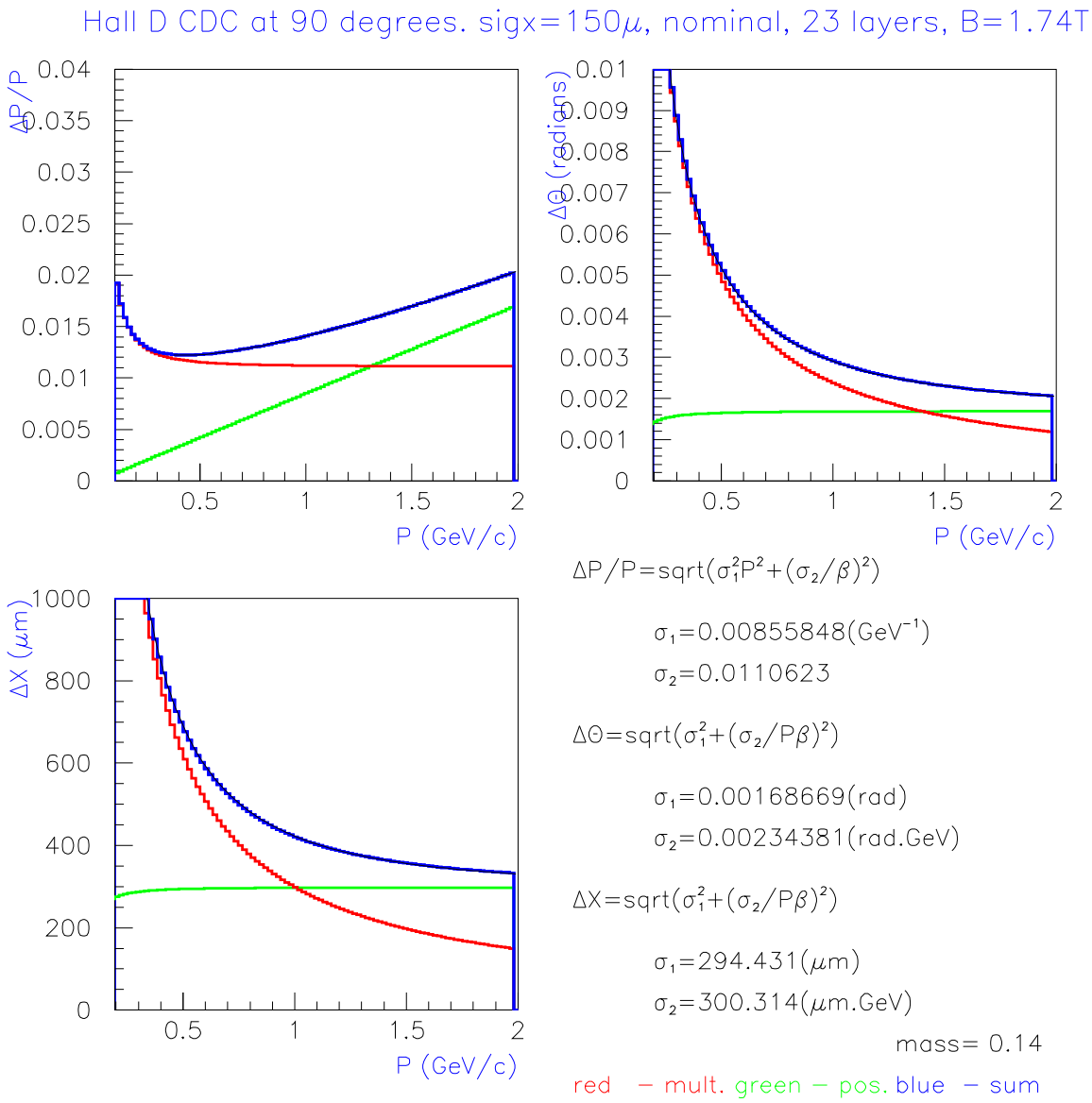

Figure 5: Momentum, angle and vertex resolution for pions as a function of momentum for the nominal configuration. The multiple scattering and position terms are plotted separately and in combination. Also given are the parameterizations of the resolution for the three variables for the nominal configuration.

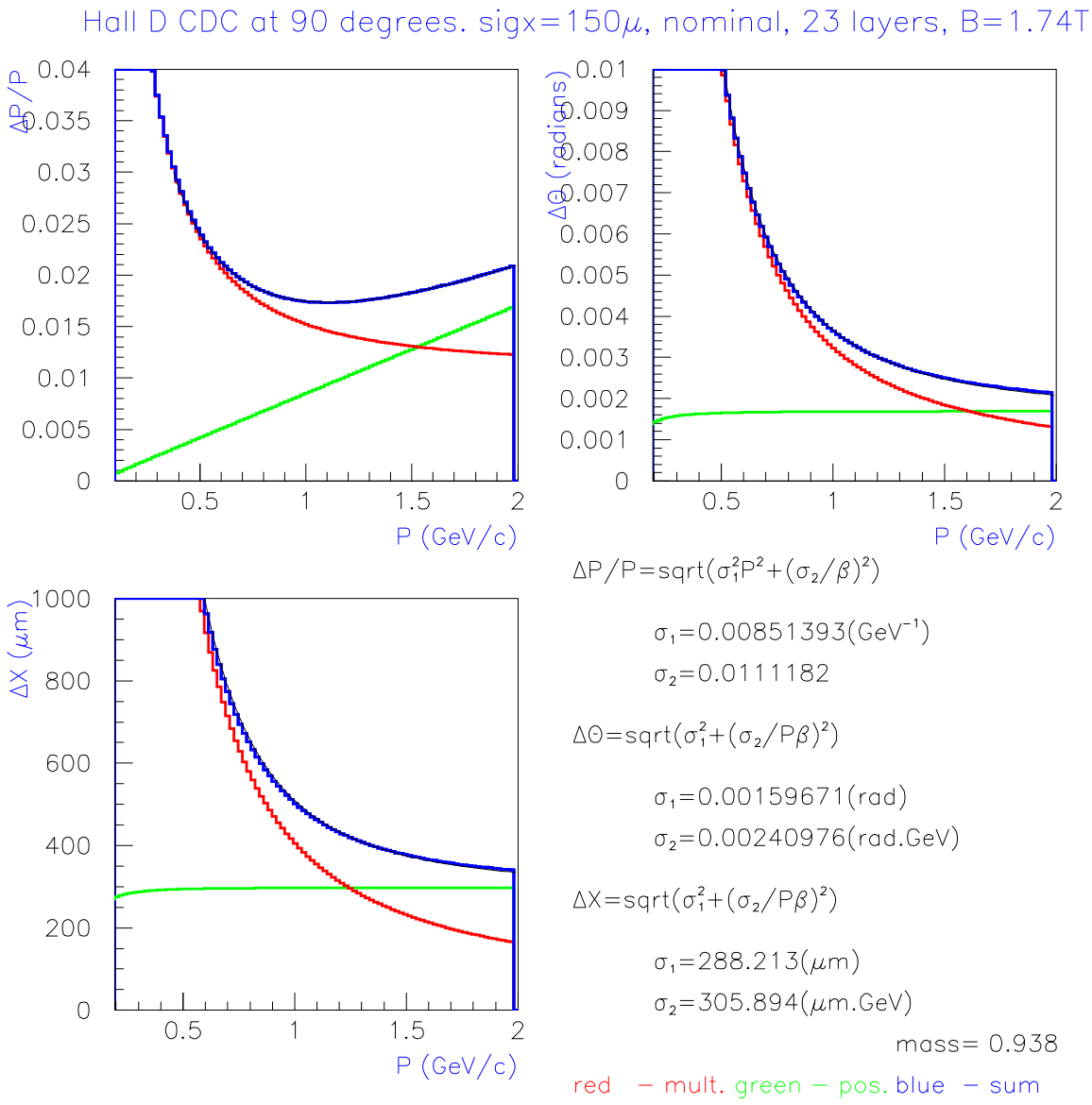

Figure 6: Momentum, angle and vertex resolution for protons as a function of momentum for the nominal configuration. The multiple scattering and position terms are plotted separately and in combination. Also given are the parameterizations of the resolution for the three variables for the nominal configuration.

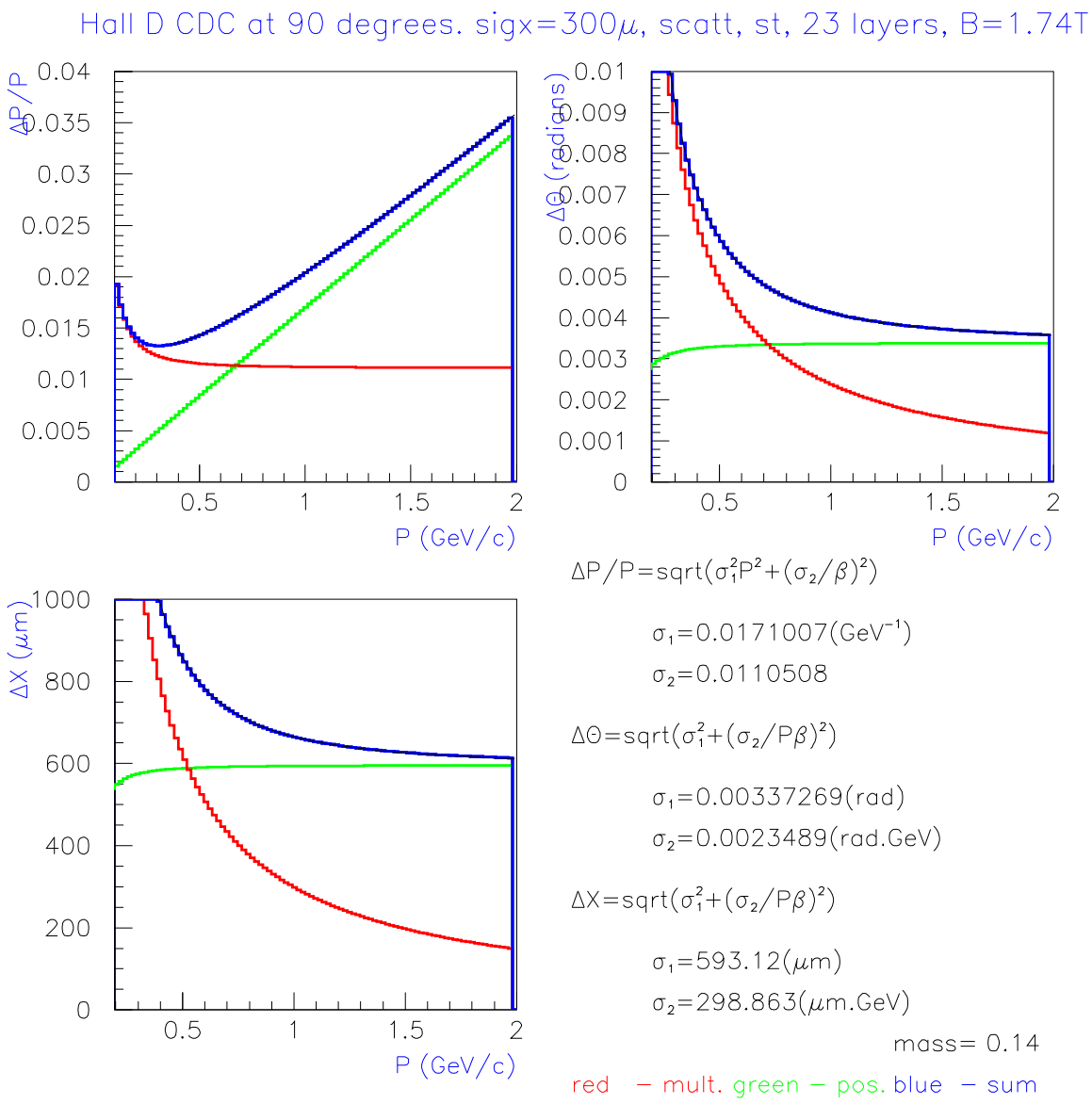

Figure 7: Momentum, angle and vertex resolution for pions as a function of momentum, assuming a chamber resolution of $\sigma = 300\mu m$. The multiple scattering and position terms are plotted separately and in combination. Also given are the parameterizations of the resolution for the three variables for this configuration. Comparison of these plots with Fig. 5 graphically show the effect of decreased position resolution in the chambers.

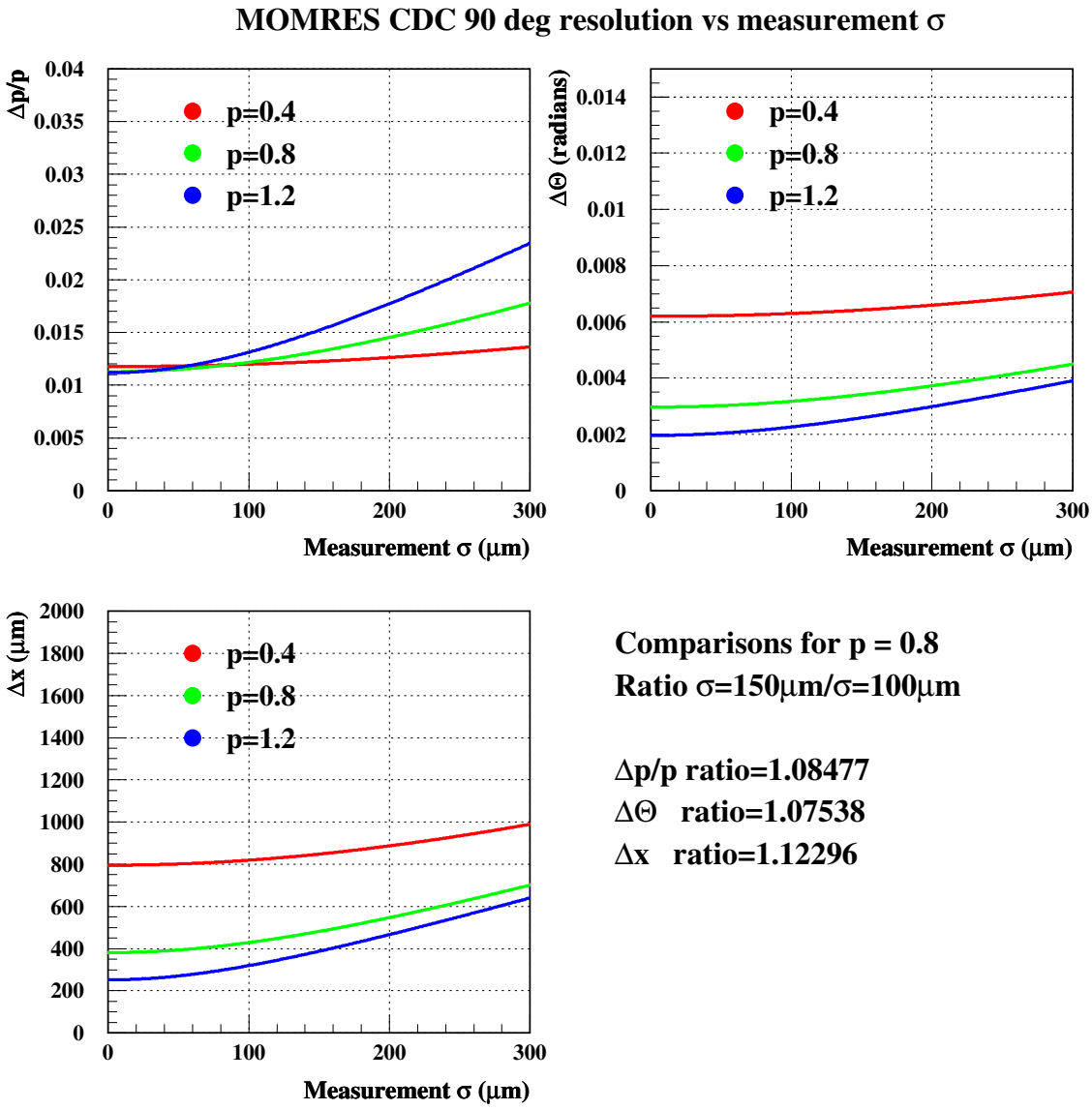

Figure 8: Momentum, angle and vertex resolution for pions as a function of measurement uncertainties in the chambers for three different momenta. Also indicated are the ratios of resolutions for the nominal uncertainties of $\sigma = 150\mu m$ compared to an improved $\sigma = 100\mu m$ at p=0.8 GeV/c. The improvements in resolutions are less than 12% when the position resolution is reduced below its nominal value.

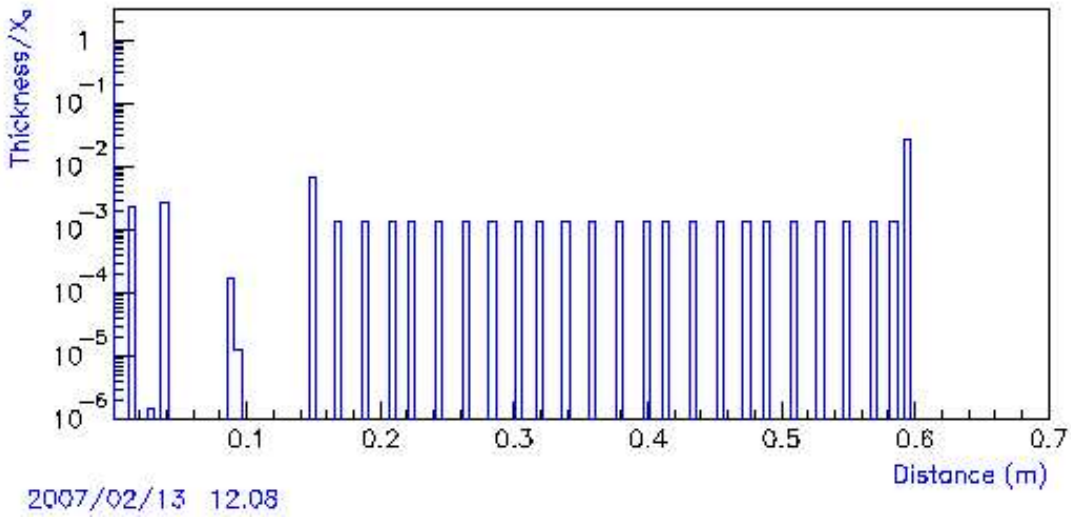

Figure 9: Distribution of material in the CDC radially replacing the start counter with air. Except for the start counter, this is the nominal configuration.

and vertex resolutions decrease by 14% and 8% respectively. Reducing the material inside the CDC to a minimal (See Fig.12) reduces these latter multiple scattering contributions by 17% and 9% compared to nominal.

7 Study of number of layers

A simple study was carried out to determine the improvement in resolution which could be achieved by adding more tracking layers close to the target. The configuration file for this study is given in Appendix B. It is likely that with the start counter in its present position it might be difficult to add three more layers, but the software allows for this. The program was re-run adding one layer at a time and the resolution parameters were plotted in Fig. 13. The position term for momentum, angular and vertex resolutions decreases linearly. The multiple multiple scattering term is approximately constant for momentum and angle, but also decreases in its contribution to the vertex position. The net effect of adding three more layers inside the nominal inner radius is that at p = 1 GeV/c the fractional momentum resolution decreases from 1.44% to 1.24%, angular resolution from 2.9 mrad to 2.5 mrad, and vertex position from 424 μ to 296 μ. It is clear that we should add as many layers close to the beam as practical due to geometrical constraints and operational rate limitations in the chambers.

8 Scaling the result to other angles

We can approximate the resolution of the perpendicular momentum for tracks at other angles in the CDC in the following way. The position term should remain unchanged

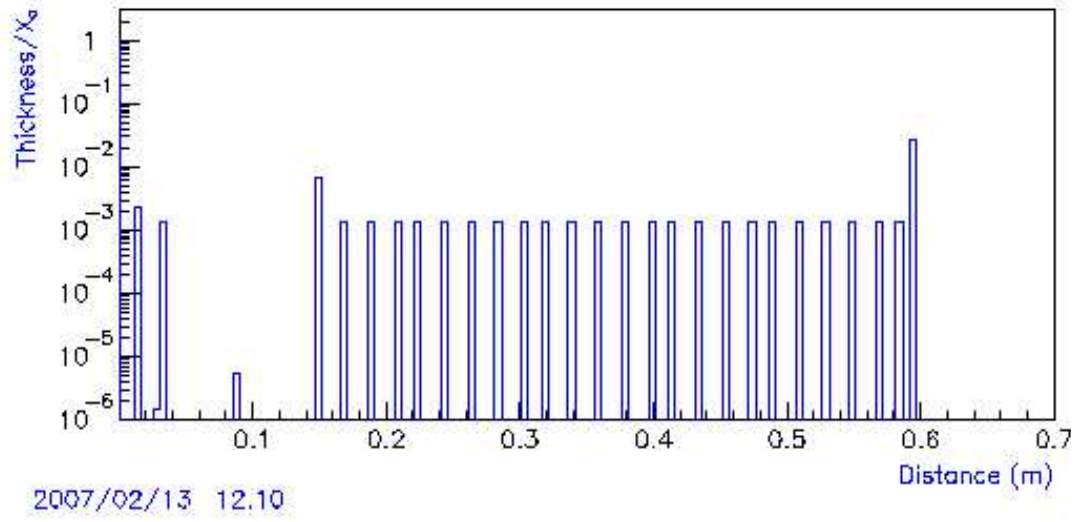

Figure 10: Distribution of material in the CDC radially outward assuming minimal material between the target and the CDC. The hydrogen target is unchanged from the nominal configuration, but vacuum extends all the way to the CDC and the foam scattering chamber thickness is halved.

but applies only to the transverse component of momentum, since no estimate is made in this approximation for the parallel component. The multiple scattering term is of the following form:

$$\frac{\delta p_\perp}{p_\perp} \propto \frac{\theta_{ms}}{\theta_{bend}} \tag{1}$$

$$\frac{\delta p_\perp}{p_\perp}(L') \propto \left(\frac{1}{p\beta}\sqrt{\frac{L'}{X_0}}\right)\left(\frac{p}{BL'}\right), \tag{2}$$

where B is the magnetic field strength and L' is the distance between the first and last measurements. If we take the angle α of the track relative to the normal incidence (i.e. 90° corresponds to α=0), then the projection of the angles onto the bend plane will be:

$$\theta_{ms}(L) = \theta_{ms}(L')/\cos\alpha \tag{3}$$

$$\theta_{bend}(L) = \theta_{bend}(L'), \tag{4}$$

where $L = L'\cos\alpha$ is projected onto the bend plane. The bend angle remains unchanged because both p and L scale as $\cos\alpha$. Thus we conclude that

$$\frac{\delta p_\perp}{p_\perp}(L) \propto \left(\frac{\cos\alpha}{p_\perp\beta}\sqrt{\frac{L/\cos\alpha}{X_0}}\cdot\frac{1}{\cos\alpha}\right)\left(\frac{p_\perp}{BL}\right) \tag{5}$$

$$\frac{\delta p_\perp}{p_\perp}(L) \propto \left(\frac{1}{\beta}\sqrt{\frac{L}{X_0}}\right)\left(\frac{1}{BL}\right)\cdot\left(\frac{1}{\sqrt{\cos\alpha}}\right) \tag{6}$$

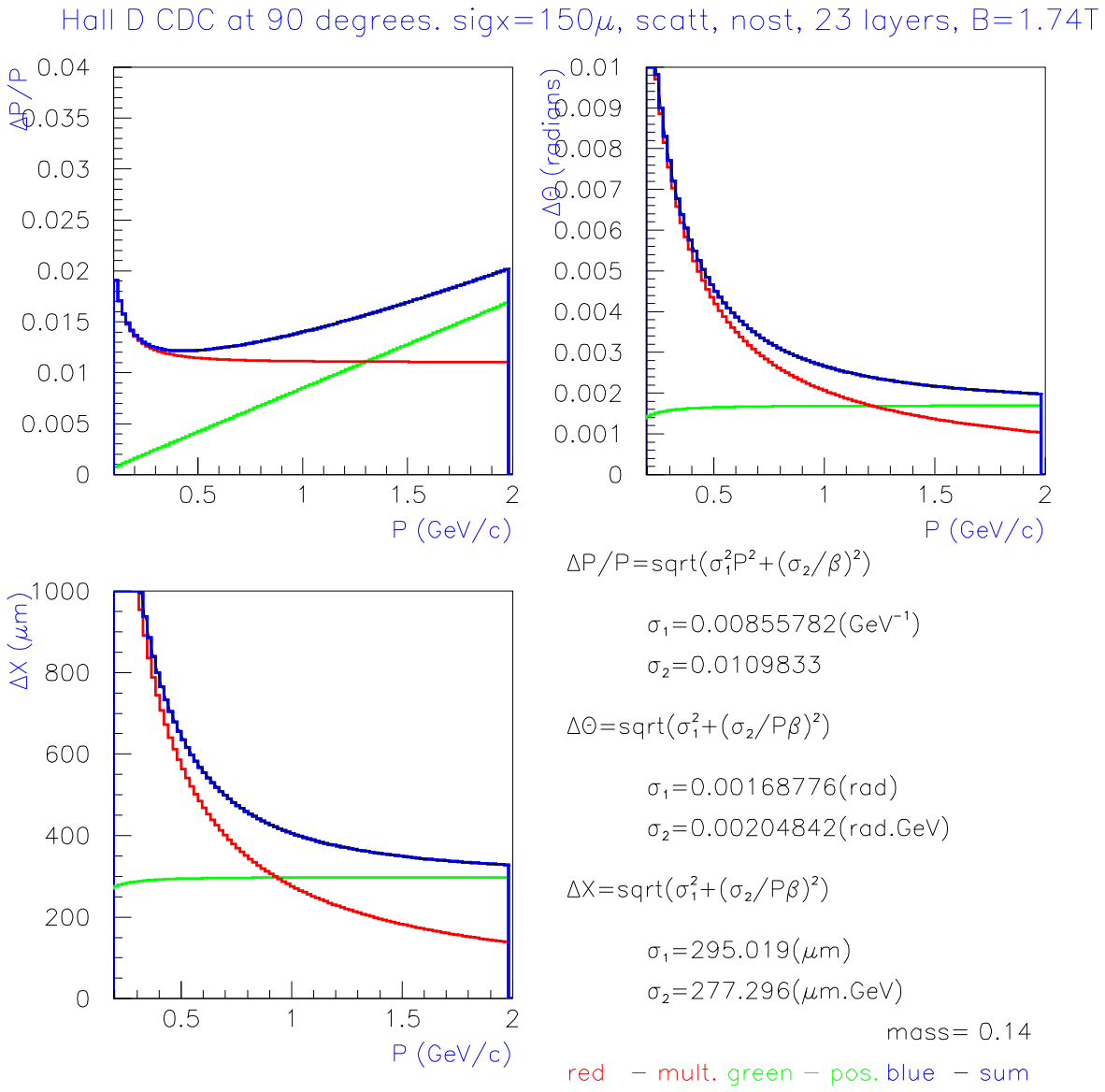

Figure 11: Momentum, angle and vertex resolution for pions as a function of momentum, replacing the material in the start counter with air. The multiple scattering and position terms are plotted separately and in combination. Also given are the parameterizations of the resolution for the three variables for this configuration. Comparison of these plots with Fig. 5 graphically show the effect of eliminating the material in the start counter.

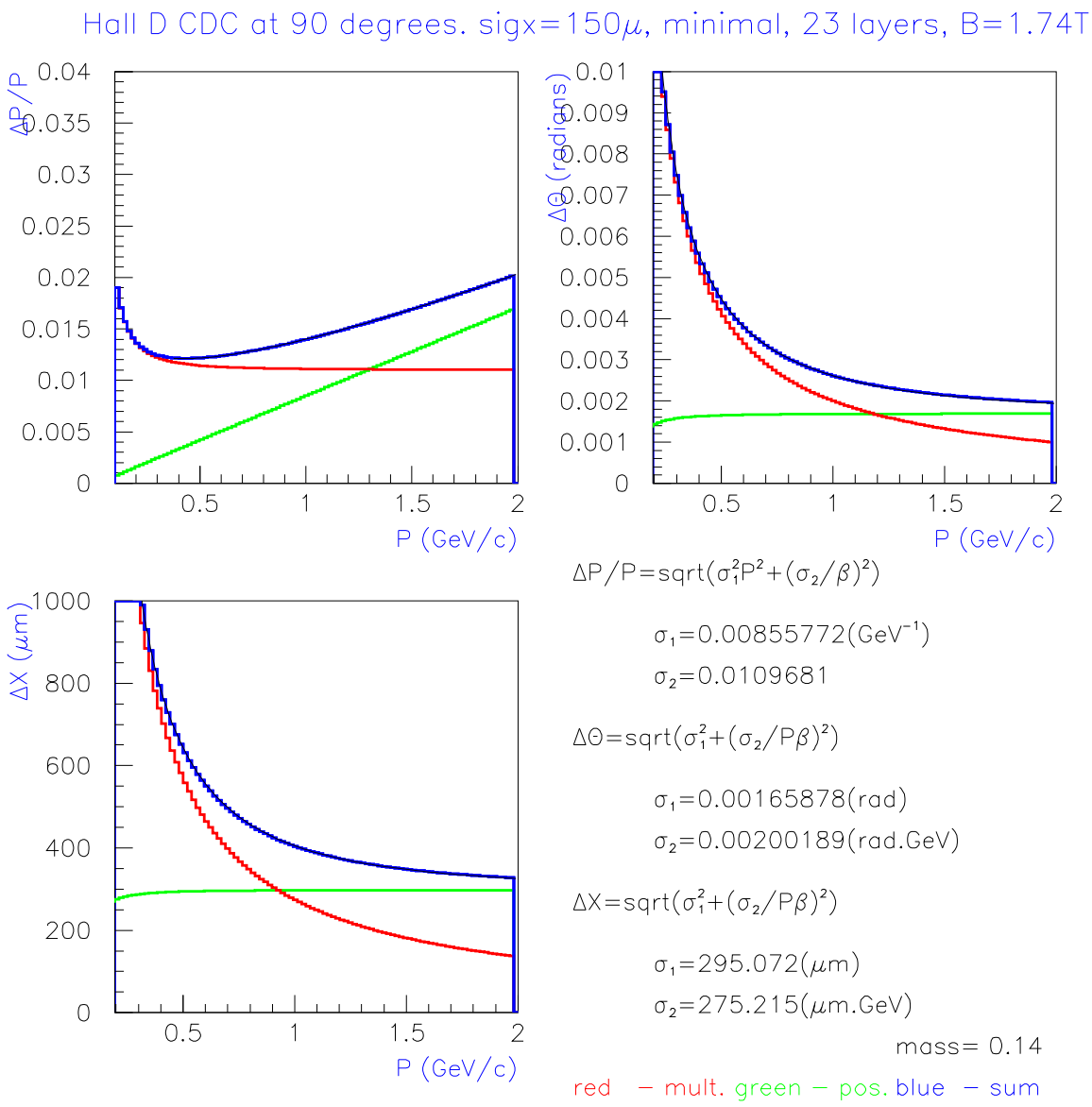

Figure 12: Momentum, angle and vertex resolution for pions as a function of momentum, assuming minimal materials inside the CDC. The multiple scattering and position terms are plotted separately and in combination. Also given are the parameterizations of the resolution for the three variables for this configuration. Comparison of these plots with Fig. 5 graphically show the effect of eliminating essentially all material inside the CDC.

With the definition that $\theta = 90 - \alpha$, then

$$\left(\frac{\delta p}{p}\right)^2 = \left(\frac{\delta p_\perp}{p_\perp}\right)^2 + \left(\frac{\delta\theta}{\tan\theta}\right)^2 \tag{7}$$

$$\left(\frac{\delta p}{p}\right)^2 = \left(\frac{\delta p}{p}\right)^2_{90^\circ} \left(\frac{1}{\sin\theta}\right) + \left(\frac{\delta\theta}{\tan\theta}\right)^2 \tag{8}$$

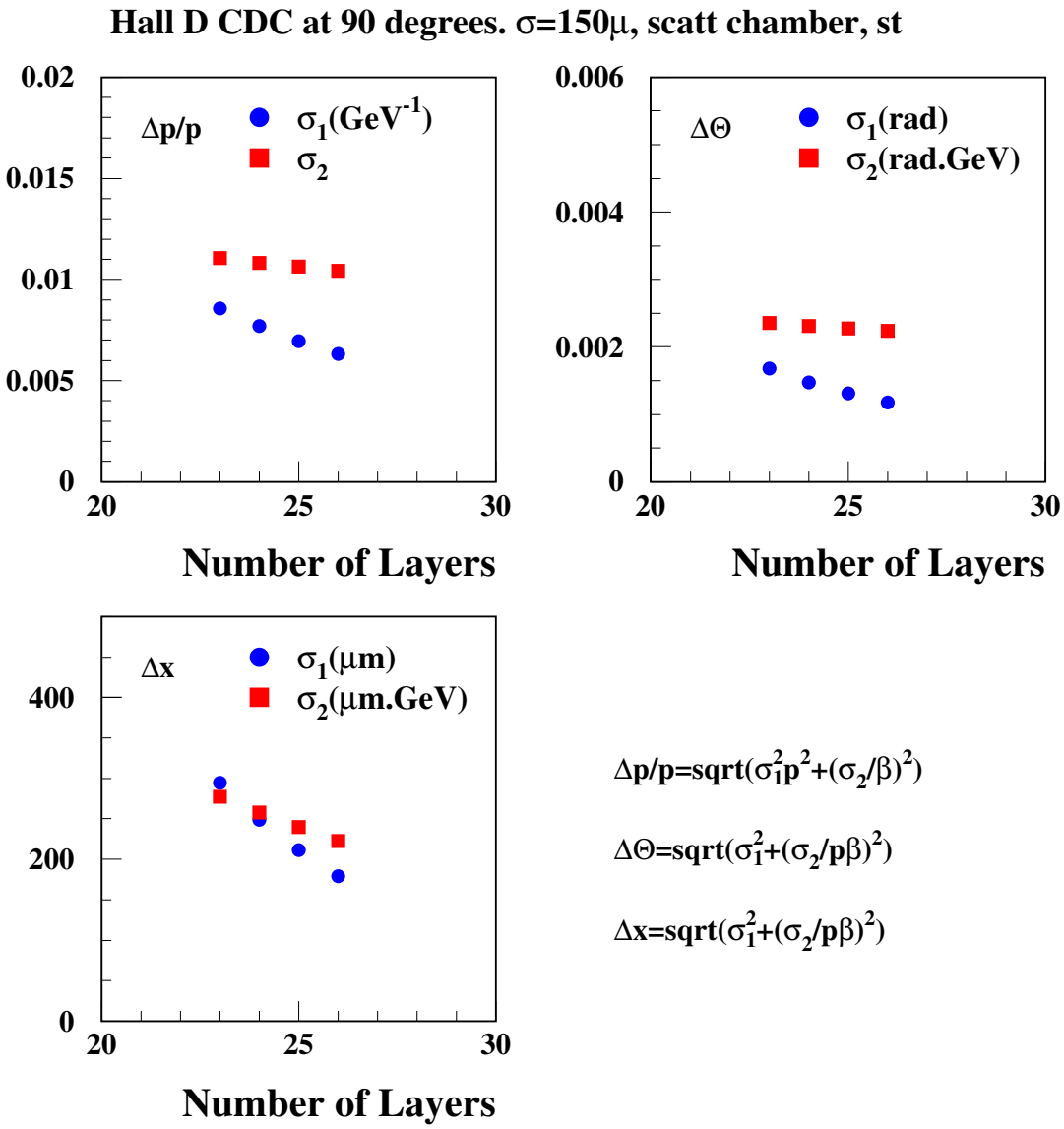

Figure 13: The multiple scattering and position terms in the resolution for pions are plotted as a function of the number of layers in the CDC. The position term for momentum, angular and vertex resolutions decreases linearly. The multiple multiple scattering term is approximately constant for momentum and angle, but also decreases in its contribution to the vertex resolution.

A Momres input file for nominal configuration

```
Input file for Main   M O M R E S
Hall D CDC at 90 degrees; sigmax=150mu, scatt chamber, st, 23 layers of straws

          1         2         3         4         5         6         7
01234567890123456789012345678901234567890123456789012345678901234567890123456
.140      0.1       2.
NR.  SS        sigma     X0        Comment
001  0.00000                      Starting coordinate
001  0.00000                      vertex constraint
002  0.01500             8.66     LH2 target
001  0.01515             0.29     Target cell wall
003  0.03000             9999.0   vacuum
001  0.04000             3.73     Rohacell scattering chamber
005  0.09000             304.00   air
001  0.09388             0.41     Start counter
005  0.14940             304.00   air
001  0.15000             0.09     CDC inner shell
001  0.16895   0.00015   13.77    CDC1
001  0.18791   0.00015   13.77    CDC2
001  0.20687   0.00015   13.77    CDC3
001  0.22582   0.00015   13.77    CDC4
001  0.24478   0.00015   13.77    CDC5
001  0.26373   0.00015   13.77    CDC6
001  0.28269   0.00015   13.77    CDC7
001  0.30165   0.00015   13.77    CDC8
001  0.32060   0.00015   13.77    CDC9
001  0.33956   0.00015   13.77    CDC10
001  0.35852   0.00015   13.77    CDC11
001  0.37747   0.00015   13.77    CDC12
001  0.39643   0.00015   13.77    CDC13
001  0.41539   0.00015   13.77    CDC14
001  0.43434   0.00015   13.77    CDC15
001  0.45330   0.00015   13.77    CDC16
001  0.47226   0.00015   13.77    CDC17
001  0.49121   0.00015   13.77    CDC18
001  0.51017   0.00015   13.77    CDC19
001  0.52913   0.00015   13.77    CDC20
001  0.54808   0.00015   13.77    CDC21
001  0.56704   0.00015   13.77    CDC22
001  0.58600   0.00015   13.77    CDC23
001  0.59200             0.22     CDC outer shell
```

B Momres input file for 26 layer configuration

```
Input file for Main   M O M R E S
Hall D CDC at 90 degrees; sigmax=150mu, scatt chamber, st, 26 layers of straws
          1         2         3         4         5         6         7
01234567890123456789012345678901234567890123456789012345678901234567890123456
.140      0.1       2.
NR.  SS        sigma     X0        relative step size, end position (m), sigma(m), ra
001  0.00000                      Starting coordinate
001  0.00000                      vertex constraint
002  0.01500             8.66     LH2 target
001  0.01515             0.29     Target cell wall
003  0.03000             9999.0   vacuum
001  0.04000             3.73     Rohacell scattering chamber
005  0.09000             304.00   air
001  0.09388             0.41     Start counter
005  0.09390             304.00   air
001  0.09450             0.09     CDC inner shell
001  0.11209   0.00015   13.77    CDC-2
001  0.13104   0.00015   13.77    CDC-1
001  0.15000   0.00015   13.77    CDC0
001  0.16895   0.00015   13.77    CDC1
001  0.18791   0.00015   13.77    CDC2
001  0.20687   0.00015   13.77    CDC3
001  0.22582   0.00015   13.77    CDC4
001  0.24478   0.00015   13.77    CDC5
001  0.26373   0.00015   13.77    CDC6
001  0.28269   0.00015   13.77    CDC7
001  0.30165   0.00015   13.77    CDC8
001  0.32060   0.00015   13.77    CDC9
001  0.33956   0.00015   13.77    CDC10
001  0.35852   0.00015   13.77    CDC11
001  0.37747   0.00015   13.77    CDC12
001  0.39643   0.00015   13.77    CDC13
001  0.41539   0.00015   13.77    CDC14
001  0.43434   0.00015   13.77    CDC15
001  0.45330   0.00015   13.77    CDC16
001  0.47226   0.00015   13.77    CDC17
001  0.49121   0.00015   13.77    CDC18
001  0.51017   0.00015   13.77    CDC19
001  0.52913   0.00015   13.77    CDC20
001  0.54808   0.00015   13.77    CDC21
001  0.56704   0.00015   13.77    CDC22
001  0.58600   0.00015   13.77    CDC23
001  0.59200             0.22     CDC outer shell
```

References

[1] B.A. Mecking. On the accuracy of track reconstruciton with inhomogeneous magnetic detectors. *Nucl. Instr. and Meth.*, 203:299, 1982.

[2] Mikhaylov, K. New results for CLAS12 parametric simulations. http://www.jlab.org/∼kmikhail/12Up/12up_22apr.ppt, 2005.

[3] Curtis Meyer. A Study of Vertex Resolution in GlueX. GlueX-doc-264, 2004.

[4] Joachim Kuhn and Curtis Meyer. Acceptance Study for the GlueX detector system. GlueX-doc-388, 2004.

[5] D. Lawrence. Charged Particle Tracking Software summary for PAC30. GlueX-doc-658, 2006.